THE
PHYSICAL REVIEW

A journal of experimental and theoretical physics established by E. L. Nichols in 1893

SECOND SERIES, VOL. 174, NO. 2 10 OCTOBER 1968

Coulomb-Recoil-Implantation Mössbauer Experiments with ^{73}Ge†

GORDON CZJZEK,* J. L. C. FORD, JR., JOHN C. LOVE,‡ FELIX E. OBENSHAIN, AND HORST H. F. WEGENER§
Oak Ridge National Laboratory, Oak Ridge, Tennessee

(Received 5 April 1968)

The 67.03-keV state of ^{73}Ge has been populated by Coulomb excitation and the recoiling excited nuclei implanted into Cr, Fe, and Cu backings. Nuclear and solid-state properties of ^{73}Ge have been determined by studying the de-excitation γ rays by Mössbauer techniques. The present measurements yield a lifetime of $(2.68\pm0.14)\times10^{-9}$ sec, and favor a spin of $\frac{5}{2}$ for the 67.03-keV excited state. The measured isomer shift between pure germanium and GeO_2 is $+1.0\pm0.1$ mm/sec, and electron densities calculated for these two cases imply that the radius of the excited state is larger than that of the ground state, and $\Delta R/R=+0.9\times10^{-3}$ in reasonable agreement with calculations based on the pairing-plus-quadrupole model. To calculate the recoilless fraction f of an impurity atom, a simple model with spring forces between nearest neighbors is introduced. In each case the effective spring constant for the impurity, as derived from the observed f value, is weaker than that of the host lattice. A remarkable difference was found between f values for tetragonal and hexagonal GeO_2, namely $f(\text{tetr})\sim5f(\text{hex})$.

I. INTRODUCTION

IT has been established that it is feasible to directly populate Mössbauer energy levels by nuclear reactions[1–6] or Coulomb excitation[7–12] and to observe the Mössbauer effect using the de-excitation radiation. These techniques not only make new nuclear levels available for traditional Mössbauer studies in addition to those populated by radioactive decay, but also provide a significant new tool for the investigation of fields such as that of radiation damage.

Although populating excited states by Coulomb excitation or nuclear reactions extends the number of Mössbauer nuclei, the observed effect may in some cases be small due to the damage of the target produced by the incident beam. Our first Mössbauer data following Coulomb excitation of ^{73}Ge,[9] for example, indicated a recoilless fraction for the target at least a factor of five smaller than the value expected from the Debye temperature. However, the Coulomb-recoil-implantation technique first applied to perturbed angular correlation experiments[13–15] has been recently used in conjunction with the Mössbauer effect.[16,17] The Coulomb-recoil-implantation Mössbauer effect (CRIME) not only provides a wider selection of host materials for a given target nucleus, but also in favorable cases is a means

† Research sponsored by the U.S. Atomic Energy Commission under contract with the Union Carbide Corporation.

* On leave 1967–1968, Kernforschungszentrum, Karlsruhe, Germany.

‡ Oak Ridge Graduate Fellow from Ohio State University under appointment with Oak Ridge Associated Universities.

§ Permanent address: Universitat Erlangen-Nurnberg, Germany.

[1] S. L. Ruby and R. E. Holland, Phys. Rev. Letters **14**, 591 (1965).

[2] D. W. Hafemeister and E. B. Shera, Phys. Rev. Letters **14**, 593 (1965).

[3] D. A. Goldberg, P. W. Keaton, Jr., Y. K. Lee, L. Madansky, and J. C. Walker, Phys. Rev. Letters **15**, 418 (1965).

[4] J. Fink and P. Kienle, Phys. Letters **17**, 326 (1965).

[5] J. Christiansen, E. Recknagel, and G. Weyer, Phys. Letters **20**, 46 (1966).

[6] J. Christiansen, P. Hendennack, V. Morfeld, E. Recknagel, D. Riegel, and G. Weyer, Nucl. Phys. **A99**, 345 (1967).

[7] D. Seyboth, F. E. Obenshain, and G. Czjzek, Phys. Rev. Letters **14**, 954 (1965).

[8] Y. K. Lee, P. W. Keaton, Jr., E. T. Ritter, and J. C. Walker, Phys. Rev. Letters **14**, 957 (1965).

[9] G. Czjzek, J. L. C. Ford, Jr., F. E. Obenshain, and D. Seyboth, Phys. Letters **19**, 673 (1966).

[10] J. Eck, Y. K. Lee, E. T. Ritter, R. R. Stevens, Jr., and J. C. Walker, Phys. Rev. Letters **17**, 120 (1966).

[11] E. T. Ritter, P. W. Keaton, Jr., Y. K. Lee, R. R. Stevens, Jr., and J. C. Walker, Phys. Rev. **154**, 287 (1967).

[12] R. R. Stevens, Jr., J. S. Eck, E. T. Ritter, Y. K. Lee, and J. C. Walker, Phys. Rev. **158**, 1118 (1967).

[13] G. Goldring, R. Kalish, and H. Spehl, Nucl. Phys. **80**, 33 (1966).

[14] L. Grodzins, R. Borchers, and G. B. Hagemann, Phys. Letters **21**, 214 (1966).

[15] F. Boehm, G. B. Hagemann, and A. Winther, Phys. Letters **21**, 217 (1966).

[16] Gordon Czjzek, J. L. C. Ford, Jr., John C. Love, Felix E. Obenshain, and Horst H. F. Wegener, Phys. Rev. Letters **18**, 529 (1967).

[17] G. D. Spouse, G. M. Kalvius, and S. S. Hanna, Phys. Rev. Letters **18**, 1041 (1967).

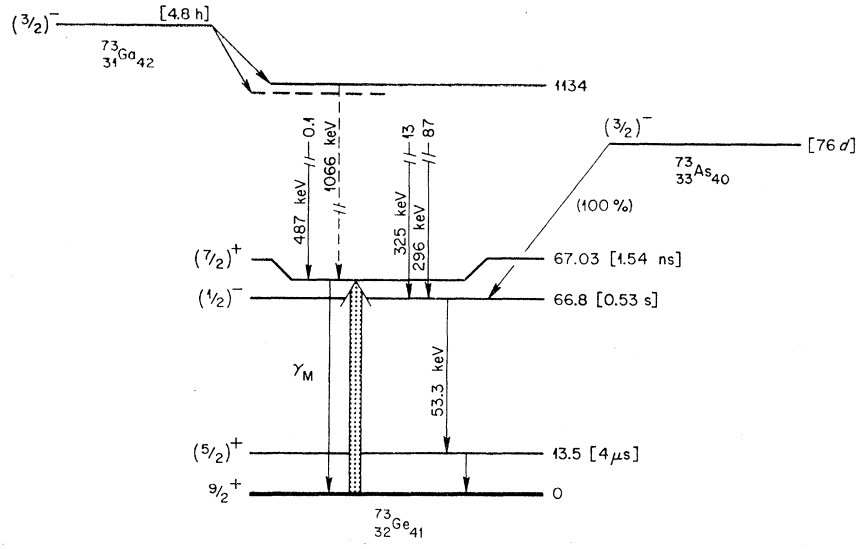

FIG. 1. Energy level scheme for the ^{73}Ge nucleus. The transition indicated by γ_M is from the relevant Mössbauer level used in the present measurements.

of avoiding effects due to background radiation, beam heating, and radiation damage.[17] The range of application of particle-induced Mössbauer experiments is therefore extended, furnishing information about solid-state and nuclear properties not obtainable by perturbed angular correlation measurements following recoil implantation or by other means.

The ^{73}Ge nucleus, whose energy level diagram is shown in Fig. 1, is a case where the Mössbauer effect has only been seen after Coulomb excitation.[9] The Mössbauer effect for γ rays from this nucleus has not been previously observed for the following reasons: The 13.5-keV first excited state has an internal conversion coefficient the order of 1000.[18,19] The lifetime of this state is about 4.0×10^{-6} sec[18] and would result in an extremely narrow Mössbauer line. The 66.8-keV state is populated through radioactive decay,[20] but this state has a 0.53-sec half-life and decays predominantly to the 13.5-keV level. The 67.03-keV state is only weakly populated by ^{73}Ga decay. No other transitions to the ground state are known which have low enough energy to be suitable for Mössbauer experiments.

Early Coulomb-excitation work suggested a spin of either $\frac{9}{2}$ or $\frac{11}{2}$ for the 67.03-keV state,[21] and we adopted the latter value in previous publications.[9,16] A more recent angular distribution measurement favors a spin $\frac{7}{2}$, while $\frac{9}{2}$ but not $\frac{11}{2}$ is excluded.[22]

In the present investigation the Mössbauer effect has been observed after the Coulomb-excited ^{73}Ge nucleus had been transplanted into Cr, Fe, and Cu backings. Section II of the paper describes the experimental techniques used and some details of the implantation process. The analysis of part of the present data was complicated by line broadening, and by the necessity of treating the Mössbauer atom as an impurity in a host lattice. A theoretical treatment of these problems is given in Sec. III in order to be able to discuss the data. The simple treatment derived here for the impurity problem yields good agreement with results computed using the more exact but laborious Green's-function formalism.[23–25] Several other simple impurity models have been published.[26] In Sec. IV the experimental data are described and solid-state and nuclear properties deduced using the approximations made in Sec. III. The deduced nuclear properties are compared with the predictions of various nuclear models in Sec. V.

II. EXPERIMENTAL METHOD

A. Equipment

The measurement of the Mössbauer effect after Coulomb excitation proceeds in the same way as a "normal" measurement when the relevant levels are populated through β decay or K capture, and the same basic criteria must be met. The source is replaced, however, by a target containing the same isotope as contained in the absorber and bombarding ions are supplied by an accelerator. Since nuclear reactions may

[18] *Nuclear Data Sheets*, compiled by K. Way *et al.* (Printing and Publishing Office, National Academy of Science, National Research Council, Washington 25, D.C.), NRC 59-1-38.
[19] R. S. Hager and E. C. Seltzer, Nucl. Data **4**, 1 (1968).
[20] F. Schweizer, G. W. Eakins, and J. Vankinken, Bull. Am. Phys. Soc. **11**, 458 (1966).
[21] G. M. Temmer and N. P. Heydenburg, Phys. Rev. **104**, 967 (1956).
[22] R. C. Ritter, P. H. Stelson, F. K. McGowan, and R. L. Robinson, Phys. Rev. **128**, 2320 (1962).
[23] A. A. Maradudin and P. A. Flinn, Phys. Rev. **126**, 2059 (1962).
[24] A. A. Maradudin, Rev. Mod. Phys. **36**, 417 (1964).
[25] A. A. Maradudin, Solid State Phys. **18**, 273 (1966); **19**, 1 (1966). These two articles extensively reference publications prior to 1966.
[26] H. L. Lipkin, Ann. Phys. (N.Y.) **23**, 28 (1963); Yu. Kagan and Ya. Iosilevskii, Zh. Eksperim. i Teor. Fiz. **44**, 284 (1963) [English transl.: Soviet Phys.—JETP **17**, 195 (1963)]; W. M. Visscher, Phys. Rev. **129**, 28 (1963); Y. Hazony, J. Chem. Phys. **45**, 2664 (1966).

contribute to the over-all background radiation, the beam energy should be kept below the Coulomb barrier. In Fig. 2 the target chamber containing liquid nitrogen is shown. The accelerator beam enters from the left and strikes a fixed target which is held near liquid-nitrogen temperature. The exact temperature will depend on the beam current and energy as well as the target contact to the liquid-nitrogen bath. However, the temperature increase above 78°K never exceeded more than a few degrees.

The targets were prepared by evaporation of the Mössbauer isotope (~80% enrichment of ^{73}Ge) onto a suitable backing material. For a sufficiently thin target the recoil of the Coulomb-excited nuclei will transplant the nucleus into the backing or host material. In the present experiment the germanium layers were of the order of 300 μg/cm^2. The implantation technique is discussed in the following section.

The target vacuum space and the absorber space which contains exchange gas are separated by a thin window (aluminum or Mylar). The temperature of the absorber may be varied by a heater arrangement from ~78 to ~250°K. The absorber is moved sinusoidally by an electromechanical device equipped with three driving coils and one velocity pickup coil. The whole system is operated in the pulse-height mode. With the sinusoidal motion it is convenient to store the Mössbauer spectrum in one memory bank of the multichannel analyzer and a nonresonant background spectrum in the second bank of the memory. Since the background spectrum is characteristic of the motion of the velocity drive, the Mössbauer spectrum is divided by the background, channel by channel, to produce a normalized velocity spectrum. The Mössbauer and the nonresonant γ rays, both arising from Coulomb excitation in the target are detected by a NaI(Tl) crystal, located in the reentrant well of the chamber.

B. Coulomb Recoil Implantation

With the Coulomb-excitation process there is a momentum transfer from the projectile to the excited nucleus. For a beam of 25-MeV oxygen ions and for medium weight target atoms the transferred kinetic energy is several MeV. In metals like Cu, Fe, Ni, or Cr the maximum range of nuclei excited by 25-MeV oxygen ions is of the order of 10^{-4} cm and the excited nuclei come to rest in a time interval of about 10^{-12} sec. The nuclear states of interest for Mössbauer studies usually have lifetimes of 10^{-9} sec or longer, and therefore the Mössbauer transitions take place long after the nuclide has been brought to rest in the chosen backing material. In metals, the nature of the environment of the Mössbauer nucleus is affected by the last few collisions of the slowing-down process and the material chosen, but not by effects such as "heat spikes." This can be seen by the following consideration: If the energy deposited along the path of the recoiling nucleus is treated as a line source of heat, the thermal conductivity equation

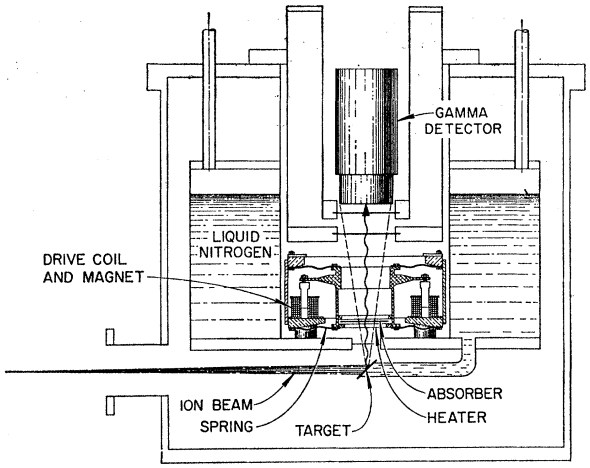

FIG. 2. Schematic of the target chamber used for Coulomb-excitation Mössbauer measurements. Source and absorber may be cooled to 78°K.

leads to a "heat pulse" which, at the final position of the Coulomb-excited nucleus, amounts to a maximum of only a few degrees for about 10^{-11} sec. The effects of such a heat pulse may be neglected.

The stopping mechanism depends upon the kinetic energy of the moving particle. In the early stages of the stopping process (for energies larger than a few keV) energy is lost mainly by electronic excitation and ionization. When the energy of the particle is reduced to a few keV the energy loss is due to phonon excitation and atomic displacements. At this stage of the slowing-down process the calculations of Vineyard *et al.*[27–29] are applicable. Their calculations show the occurrence of replacement collisions, wherein the colliding atoms exchange their roles and the Mössbauer nucleus occupies a lattice site after the collision. Because there are a large number of interactions during the slowing down process the probability for an exchange collision is nearly one.[27–30] Another result of Vineyard's calculations is that the lattice site where the excited Mössbauer atom stops is often in the neighborhood of one or more vacancies. The effect of the heat pulse does not rearrange this final configuration. Although in most of our experiments discussed in Sec. IV the Coulomb-excited atom was an impurity (^{73}Ge in Cr, Fe, Cu), the results of Vineyard's model should at least give a qualitative picture: *The excited Mössbauer atoms stop mostly on lattice sites and are often surrounded by one or two vacancies.*

Every Coulomb-excitation Mössbauer experiment may involve the process of implantation. When the

[27] J. B. Gibson, A. N. Goland, M. Milgram, and G. H. Vineyard, Phys. Rev. **120**, 1229 (1960).
[28] C. Erginsoy, G. H. Vineyard, and A. Englert, Phys. Rev. **133**, A595 (1964).
[29] C. Erginsoy, G. H. Vineyard, and A. Shimizu, Phys. Rev. **139**, A118 (1965).
[30] P. H. Dederichs, C. Lehmann, and H. Wegener, Phys. Status Solidi **8**, 213 (1965).

range of the projectile is larger than the thickness of the target material a certain fraction of the target nuclei will be transplanted into the backing material. The Coulomb-recoil-implantation technique has been used in conjunction with perturbed angular correlation measurements, where the main purpose was to transplant the target nucleus into a ferromagnetic host material.[13–15] Solid-state ring counters were used in these experiments to detect the back-scattered oxygen ions in order to select only those target nuclei with a recoil energy great enough to be implanted into the host material. It is possible to work with ring counters in Mössbauer experiments, but the high beam currents used in the present measurements made their use impractical.

Our experiments required that the implanted fraction be calculated in order to determine the recoilless fraction of the target. The implanted fraction η is defined by

$$\eta=\frac{\text{number of implanted excited nuclei}}{\text{number of excited nuclei}}$$

$$=\int_0^{d/\sin\gamma} dx\, Y(x) \int_0^{\pi/2} f(\theta, x)\sigma(\theta)\, \sin 2\theta d\theta \Big/ \int_0^{d/\sin\gamma} dx\, Y(x) \int_0^{\pi/2} \sigma(\theta)\, \sin 2\theta d\theta, \quad (1)$$

where d, x, θ, and γ are defined in Fig. 3 and $Y(x)$ is the relative γ-ray yield of nuclei excited at the depth x in the target. The fraction of nuclei recoiling in the interval $d\theta$ about θ from the depth x and transplanted into the backing material is given by $f(\theta, x)$. The function $\sigma(\theta)$ is the Coulomb-excitation differential cross section.[31] The above expression has been evaluated numerically, but with the simplifying assumptions that (1) the scattering is isotropic in the center-of-mass system and (2) the target thickness d is small compared with the maximum range R_0 of the excited nuclei in the target material, a closed form for η may be obtained. This approximate relationship is given by

$$\eta\cong\tfrac{1}{2}(1+\sin\gamma)-\frac{d}{3R_0}\left(\frac{3R_p\sin\gamma-d}{2R_p\sin\gamma-d}\right), \quad (2)$$

where R_p is the projectile range. A comparison of results calculated from Eqs. (1) and (2) is given in Table I.

III. THEORETICAL CONSIDERATIONS

A. Simple Impurity Model

In most of our experiments the Mössbauer atom was implanted as an impurity atom in a host lattice. The Debye-Waller factor f is then a complicated function of the interatomic forces, the impurity mass M, and mass M_0 of the host-lattice atoms. The problem of an impurity atom in a host material has been studied[25,26] but the application of the exact formula for the resulting recoilless fraction $f(T)$ is often too laborious to be justified. We prefer therefore to discuss our data in the framework of a simple impurity model, which simplifies the computation. A detailed description of the model will be published elsewhere.[32]

Neglecting localized modes and nonharmonic terms in the lattice potential energy, the recoilless fraction $f(T)$ for γ radiation emitted in the x direction is related to the mean square of the x displacement of the Mössbauer atom[33]:

$$-\lambda\!\!\!^{-2}\ln f(T)=\langle x^2\rangle_T, \quad (3)$$

where $\lambda\!\!\!^{-}$ is the γ-ray wavelength divided by 2π and T the absolute temperature. In our model we consider the n nearest neighbors of the Mössbauer impurity as a cage in which the impurity is captured. The potential within the cage is nearly spherically symmetric because of the large number of equally distributed nearest neighbors. The motion of the Mössbauer atom in the cage can thus approximately be considered as that of a three-dimensional Einstein oscillator with a (quasi-constant) frequency Ω. The motion of the cage as a whole is determined by the low-frequency elastic waves of the host crystal. Two forces act on the impurity within the cage: (a) the force F_a due to the "spring" of the Einstein oscillator and (b) the inertial force F_b due to the motion of the cage. In thermal equilibrium

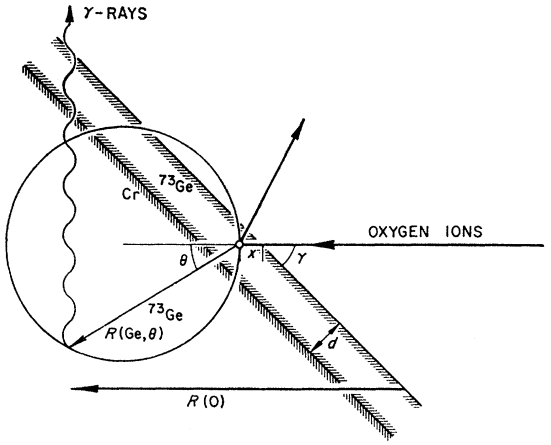

FIG. 3. Diagram showing the relevant parameters and geometry for calculation of the Coulomb-recoil-implantation fraction η. The range of the Ge recoil atom is indicated by $R(\mathrm{Ge}, \theta)$.

[31] K. Alder, A. Bohr, T. Huus, B. Mottelson, and A. Winther, Rev. Mod. Phys. **28**, 432 (1956).

[32] H. H. F. Wegener, Phys. Status Solidi (to be published).

[33] Horst Wegener, *Der Mössbauer-effect und seine Anwendungen in Physik und Chemie* (Bibliographisches Institut Mannheim, Germany, 1965), Eqs. (3.79) and 3.80).

the two forces satisfy the inequality

$$|F_b/F_a| \leq (M/M_0)^{1/2}(n+1)^{-5/6} \ll 1, \quad (4)$$

as will be shown in Ref. 32. As a consequence, the motion of the impurity atom within the cage is almost independent of the motion of the cage itself, i.e., the Einstein oscillator and the low-frequency elastic waves are, practically, decoupled. To obtain the low-frequency spectrum, we have to consider the cage and the impurity as a single lattice "molecule." The N lattice atoms are arranged to give $N/(n+1)$ such molecules. The "molecular" lattice has $3N/(n+1)$ degrees of freedom specified by $3N/(n+1)$ normal modes, each characterized by a wave vector $\mathbf{q}$ and a polarization (longitudinal l or transverse t). The related vibration frequencies $\Omega_{l,t}(\mathbf{q}) = c_{l,t}q$ depend upon the elastic wave velocities c_l and c_t for the two polarizations.

Decoupling the Einstein oscillator and the "molecular" lattice eases the calculation of $\langle x^2\rangle_T$. It is simply the sum over the $\langle x^2\rangle_T$ values of the two motions. The final result can be written as follows:

$$\langle x^2\rangle_T = \frac{\hbar}{M\Omega(1+M/nM_0)}\{\tfrac{1}{2}+[\exp(\hbar\Omega/kT)-1]^{-1}\} + \frac{\hbar}{(n+1)M_0}\left[\frac{F(\hbar\varphi_l/kT)}{\varphi_l}+2\frac{F(\hbar\varphi_t/kT)}{\varphi_t}\right],$$

$$\varphi_{l,t} \equiv [6\pi^2\rho/(n+1)M_0]^{1/3}c_{l,t},$$

$$F(y) \equiv \frac{1}{y^2}\int_0^y \frac{x}{e^x-1}\,dx+\tfrac{1}{4}, \quad (5)$$

and

$$F(y) \approx 1/y+y/36, \quad \text{for } y \ll 1$$
$$\approx \tfrac{1}{4}+\pi^2/(6y^2), \quad \text{for } y \gg 1$$

where ρ is the density of the host lattice. All other symbols used in Eq. (5) were explained previously or are obvious.

To further simplify our model, let us assume that each atom is connected to its nearest n neighbors by spring forces. The spring constants are α_0 and α for the forces between two lattice atoms and between one lattice atom and the impurity, respectively. The quantities φ_l, φ_t, and Ω can then be expressed in terms of the masses and spring constants:

$$\varphi_{l,t} = a_{l,t}(\alpha_0/M_0)^{1/2},$$
$$\Omega = \left(\frac{n(n+2M/M_0)}{3(n+M/M_0)}\right)^{1/2}\left(\frac{\alpha}{M}\right)^{1/2}. \quad (6)$$

The constants a_l and a_t depend upon the lattice structure. The values of n, a_l, and a_t are 8, $[\frac{4}{3}\pi^2]^{1/3}/\sqrt{3}$, and $[\frac{4}{3}\pi^2]^{1/3}/\sqrt{3}$, respectively, for a body-centered cubic lattice, and 12, $[3\pi^2/13]^{1/3}\sqrt{2}$, and $[3\pi^2/13]^{1/3}$ for a face-centered cubic lattice.

Our model may be tested by applying it to the case of a Mössbauer atom which is not an impurity but a normal lattice atom. Then $M \to M_0$, $\alpha \to \alpha_0$ $\langle x^2\rangle_T \to \langle x_0^2\rangle_T$, and combining Eqs. (5) and (6) gives

$$\langle x_0^2\rangle_T = \hbar/(M_0\alpha_0)^{1/2}(b_0\{\tfrac{1}{2}+[\exp(c_0/\tau)-1]^{-1}\} + b_lF(a_l/\tau)+b_tF(a_t/\tau)),$$
$$\tau \equiv kT/[\hbar(\alpha_0/M_0)^{1/2}],$$
$$b_0 \equiv [3n/(n+2)(n+1)]^{1/2},$$
$$c_0 \equiv [3n(n+2)/(n+1)]^{1/2},$$
$$b_l \equiv 1/(n+1)a_l,$$
$$b_t \equiv 2/(n+1)a_t. \quad (7)$$

If the phonon spectrum $g(\Omega)$ is known, one may compute $\langle x_0^2\rangle_T$ from the well-known formula[33]

$$\langle x_0^2\rangle_T = \frac{\hbar}{M_0}\int_0^\infty \frac{g(\Omega)}{\Omega}\{\tfrac{1}{2}+[\exp(\hbar\Omega/kT)-1]^{-1}\}d\Omega. \quad (8)$$

The result of Eq. (8) is to be compared with the one obtained with the model Eq. (7). Chromium, for which $g(\Omega)$ is available,[34] is a good example. Assuming $(\alpha_0/M_0)^{1/2} = 2.69\times10^{13}$ sec^{-1}—a value compatible with the elastic constants of chromium—values for $\langle x_0^2\rangle_T$ obtained from Eqs. (7) and (8) agree to within about 1% for temperatures between 0 and 400°K.

In most of our experiments the Mössbauer atom was an impurity and the temperatures ($\geq$78°K) were sufficiently high to allow the expansion of Eq. (5) in inverse powers of T:

$$\langle x^2\rangle_T = \left[\frac{A}{\alpha}+\frac{B}{\alpha_0}\right]kT+\frac{\hbar^2}{12\mu}(kT)^{-1}+O\left(\frac{\hbar^4}{T^3}\right),$$

$$A \equiv \frac{3}{n+2M/M_0} \approx \frac{3}{n+2}\left(1-2\frac{\delta M}{(n+2)M_0}\right),$$

$$\delta M \equiv M-M_0,$$

$$B \equiv (n+1)^{-1}(1/a_l^2+2/a_t^2)$$
$$= \{\alpha_0/[\pi M_0(n+1)]^{1/3}(6\rho)^{2/3}\}(1/c_l^2+2/c_t^2),$$

$$\mu^{-1} \equiv [M(1+M/(nM_0))]^{-1}+[M_0(n+1)]^{-1} \approx M^{-1}. \quad (9)$$

TABLE I. Calculated values of the implantation fraction. $R_0/R_p = 0.33$. However, η is independent of R_0/R_p in the range $0.1 \leq R_0/R_p \leq 0.5$.

d/R_0	$\gamma=45°$ η^a	$\gamma=45°$ η^b	$\gamma=75°$ η^a	$\gamma=75°$ η^b
0.1	0.73	0.80	0.86	0.90
0.2	0.66	0.75	0.79	0.85
0.3	0.58	0.70	0.71	0.80
0.4	0.52	0.64	0.64	0.75
0.5	0.45	0.59	0.56	0.70

[a] Calculated from Eq. (1) of text.
[b] Calculated from Eq. (2) of text.

[34] G. Dolling (unpublished).

To obtain Eq. (9) the spring-force model [Eq. (6)] has been used. The right-hand sides of the equations for A and $1/\mu$ are approximations up to terms of the order $1/n^2 \ll 1$. The (kT) term, the only contribution to $\langle x^2\rangle_T$ in the classical limit as $\hbar \to 0$, depends upon the spring constants α and α_0, and the lattice-structure parameters n, a_l, and a_t.[35] On the other hand, the lowest-order quantum-mechanical contribution to $\langle x^2\rangle_T$ is proportional to $\hbar^2/(kT)$, and depends upon the impurity mass M but not the spring constants. Our term $\hbar^2/(12MkT)$ agrees with that given by the exact treatment of Maradudin and Flinn in Ref. 23.

In order to compare a measured Debye-Waller factor of an impurity Mössbauer atom with that predicted by Eq. (9), we proceed as follows: From the observed recoilless fraction f and Eq. (3) we determine $\langle x^2\rangle_T$, and consequently the quantity

$$q \equiv \frac{\langle x^2\rangle_T - \hbar^2/(12\mu kT)}{kT}. \tag{10}$$

This can be compared to the q value predicted by the model of Eq. (9):

$$q = A/\alpha + B/\alpha_0 + \cdots. \tag{11}$$

The omitted terms are at least of order $1/T^3$. If the host-lattice quantity B/α_0 is known, then Eq. (11) may be used to determine the impurity spring constant α.

Instead of α it may sometimes be more instructive to know the fractional change in the spring constant $(\alpha-\alpha_0)/\alpha_0$ when a lattice atom is replaced by the impurity. As the δM term in A is generally small, we obtain from Eq. (11):

$$q = q_0\left(1+\frac{A}{A+B}\frac{\alpha_0-\alpha}{\alpha}\right)$$

$$= q_0\left[1+\frac{A}{A+B}\sum_{m=1}^{\infty}\left(\frac{\alpha_0-\alpha}{\alpha_0}\right)^m\right],$$

$$q_0 \equiv \frac{\langle x_0^2\rangle_T - \hbar^2/(12M_0kT)}{kT}, \tag{12}$$

where q_0 may be computed from Eq. (8) if the phonon spectrum $g(\Omega)$ of the host lattice is known, or otherwise from Eq. (7). For face- and body-centered cubic lattices, the ratio

$$\frac{A}{A+B} \approx \frac{1}{1+\{(n+2)/(n+1)\}\frac{1}{3}(1/a_l^2+2/a_t^2)} \tag{13}$$

is 0.66 and 0.63, respectively. Maradudin and Flinn[23] have derived a comparable q formula using the high-temperature approximation for the spring-force model of a face-centered cubic host lattice. Under the restrictive assumption $[(\alpha-\alpha_0)/\alpha_0]^2 \ll 1$, they get

$$q = q_0\left[1+0.60\,\frac{\alpha_0-\alpha}{\alpha_0}+0.74\left(\frac{\alpha_0-\alpha}{\alpha_0}\right)^2+\cdots\right]. \tag{14}$$

The numerical factors were calculated in the Ludwig approximation[36] and are thus reliable only to within about 20%. The equation obtained with our model [i.e., Eq. (12)] for a face-centered cubic lattice

$$q_{\text{fcc}} = q_0\left[1+0.66\sum_{m=1}^{\infty}\left(\frac{\alpha_0-\alpha}{\alpha_0}\right)^m\right] \tag{15}$$

is in reasonable agreement with Eq. (14), although not restricted to a small fractional change in the spring constant.

B. Magnetic Line Broadening for High-Spin Mössbauer Levels

Some of our Mössbauer spectra show a line broadening which is probably caused by a magnetic hyperfine interaction. In this case the large nuclear spins $\frac{7}{2}$ and $\frac{9}{2}$ in the excited and the ground states of ^{73}Ge permit a simple treatment of the line shape. The characteristic broadening parameter

$$\Delta \equiv 2H\,|\,\mu_e-\mu_g\,|\,\tau_n/\hbar \tag{16}$$

depends upon the magnetic field H acting upon the nucleus, the difference of the nuclear magnetic dipole moments in the excited and the ground states, and the lifetime τ_n of the excited state. We will refer to the following treatment as the Δ approximation.

The internal magnetic field H removes the $2j+1$ degeneracy of the nuclear levels. The frequency of the emitted radiation is then shifted by the following amount:

$$\delta\omega(m_e, m_g) = -(\mu_e m_e/j_e - \mu_g m_g/j_g)H/\hbar, \tag{17}$$

where j_e, j_g, m_e, and m_g are the excited-state and ground-state spins and magnetic quantum numbers, respectively. In the case of dipole radiation ($|\,j_e-j_g\,| \leq 1$, $|\,m_e-m_g\,| \leq 1$), and large j values the ratios m_e/j_e and m_g/j_g are about equal, and Eq. (17) becomes approximately

$$\delta\omega(m_e, m_g) \approx -[H(\mu_e-\mu_g)/\hbar]m_g/j_g$$

$$\equiv \delta\omega(m_g). \tag{18}$$

Let us consider a Mössbauer experiment with a single line source of natural linewidth $\Gamma = \hbar/\tau_n$ and an absorber with a magnetic hyperfine splitting according to Eq. (18). In the absorber all $2j_g+1$ possible m_g values are equally populated and if the internal field directions are random, all frequencies $\delta\omega(m_g)$ occur with equal weight. If the separation of two adjacent absorption lines is much smaller than Γ, we may approximate the discrete line positions and intensities by a continuous rectangu-

[35] The mass dependence $2\delta M/[(n+2)M_0] \ll 1$ is not significant but is a consequence of our model. The "correct" classical expression for $\langle x^2\rangle_T$ is strictly mass-independent.

[36] W. Ludwig, J. Phys. Chem. Solids **4**, 283 (1958).

lar distribution function D for the frequency shift $\delta\omega$:

$$D(\delta\omega) = \tau_n/\Delta, \quad \text{for} \quad |\delta\omega| \leq \Delta/(2\tau_n)$$
$$= 0, \quad \text{otherwise} \tag{19}$$

where we have introduced Δ from Eq. (16).

The cross section for resonance absorption is then determined by $D(\delta\omega)$ as follows [Ref. 33, Eq. (1.29)]:

$$\sigma_\Delta(\omega) = \sigma_0(\Gamma/2\hbar)^2 \int \frac{D(\delta\omega)}{(\omega-\omega_0-\delta\omega)^2+(\Gamma/2\hbar)^2}\, d(\delta\omega), \tag{20}$$

where

$$\omega_0 = (E_e - E_g)/\hbar,$$
$$\sigma_0 = [2\pi\lambda^2/(1+\alpha_{ic})](2j_e+1)/(2j_g+1),$$

and α_{ic} is the internal conversion coefficient. Introducing Eq. (19) into Eq. (20) we obtain

$$\sigma_\Delta(\omega) = \sigma_0 S_\Delta[2\tau_n(\omega-\omega_0)],$$
$$S_\Delta(x) \equiv [\arctan(\Delta+x)+\arctan(\Delta-x)]/2\Delta. \tag{21}$$

In a Mössbauer experiment the counting rate $C(v)$ of the γ rays transmitted through an absorber is measured as a function of the velocity v between source and absorber. As the counting rate due to nonresonant absorption is $C(\infty)$, it is convenient to define the ratio $M(v)$, which in the case of a single-line emission spectrum and an absorber with resonance cross section $\sigma_\Delta(\omega)$ is

$$M(v) \equiv [C(\infty)-C(v)]/C(\infty)$$
$$= \lambda^{-1} f_s \times \pi^{-1} \int_{-\infty}^{+\infty} \frac{1-\exp[-T_{\text{eff}} S_\Delta(x)]}{1+(x-2v/v_{1/2})^2}\, dx,$$
$$T_{\text{eff}} \equiv n_a f_a \sigma_0, \qquad v_{1/2} \equiv c/(\tau_n \omega_0), \tag{22}$$

where $v_{1/2}$ is the natural half-width velocity of the Mössbauer line. The effective absorber thickness T_{eff} contains n_a, the number of Mössbauer isotopes per unit area, and the Debye-Waller factor f_a of the absorber material. For a given source and in the absence of electric hyperfine interactions the largest Mössbauer effect, $M_{\max} = \lambda^{-1} f_s$, is obtained with a thick absorber $T_{\text{eff}} \approx \infty$ at $v=0$. It depends on the recoilless fraction f_s of the source and the "total to signal" ratio λ of the γ-ray detector. For a finite absorber thickness the characteristic features of a Mössbauer line are the maximum absorption $M(0)$ at zero velocity, the observed half-width velocity $V_{1/2}$, defined by the integral equation $2M(V_{1/2}) = M(0)$, and the area under the absorption curve

$$F = \int_{-\infty}^{+\infty} M(v)\, dv.$$

The area F has the useful property that it is independent of the source line shape and spectrometer velocity resolution.[37] The integral in Eq. (22) has been evaluated numerically, and the quantities $M(0)$, $V_{1/2}$, and F are displayed in Fig. 4 as functions of the absorber thickness T_{eff} for six broadening parameters: $\Delta = 0, 1, 2, 3, 4, 5$. The special case $\Delta = 0$ is well known and was discussed in detail by Margulies and Ehrmann.[38]

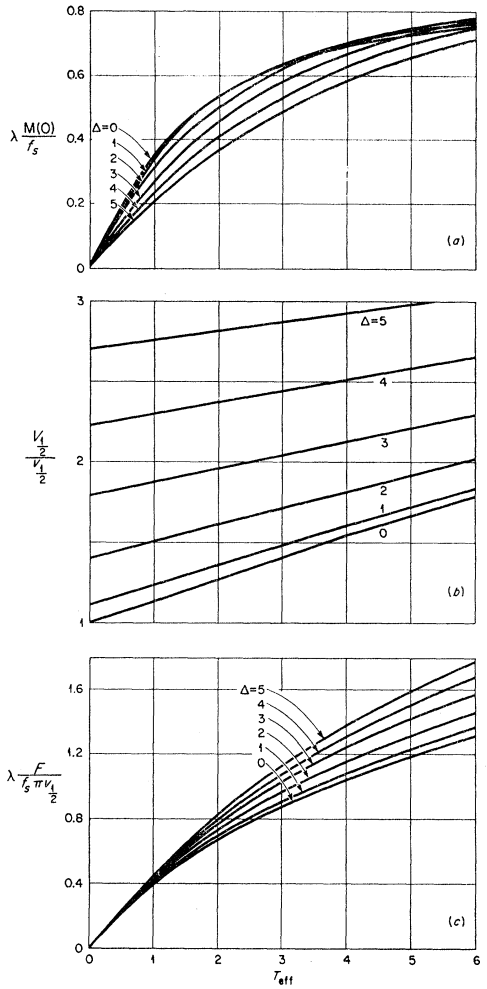

FIG. 4. Parameters characterizing a Mössbauer spectrum with unresolved magnetic hyperfine splitting in the absorber are shown as a function of effective thickness T_{eff} of the absorber. They are (a) the maximum Mössbauer effect, (b) the width of the spectrum at half-maximum, (c) the area under the spectrum. The other symbols are the broadening parameter Δ, the γ detector total to signal ratio λ, the recoilless fraction of the source f_s, and the velocity corresponding to the natural width at half-maximum, $v_{1/2}$. Here, $\Delta = 0$ corresponds to a single-line absorption spectrum.

IV. EXPERIMENTAL DATA AND COMPARISON WITH THEORY

A. Implantation Sources

The Coulomb-excited 67.03-keV radiation from ^{73}Ge showed an unexpectedly small Mössbauer effect when

[37] G. Lang, Nucl. Instr. Methods **24**, 425 (1963).

[38] S. Margulies and J. R. Ehrmann, Nucl. Instr. Methods **12**, 131 (1961).

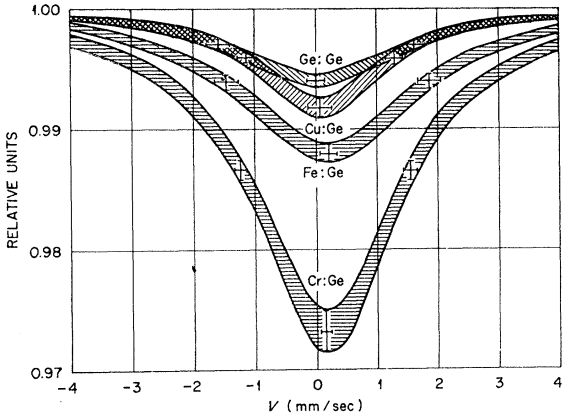

FIG. 5. The Lorentzian bands shown were derived from the actual spectra by making a least-squares fit to the data. They represent Mössbauer spectra taken with a natural germanium absorber (138-mg/cm^2 Ge) and germanium target nuclei implanted into chromium, iron, and copper. A thick germanium layer was used for the measurement labeled Ge:Ge. For each line the center position and the half-width velocities are marked. The vertical error bars indicate the uncertainties of the Mössbauer effect and the horizontal bars indicate uncertainties in the position and the width of the lines.

a thick germanium target was used.[9] An x-ray investigation of the targets before and after irradiation indicated a complete conversion from the crystalline to an amorphous state.[16] The observed recoilless fraction must certainly be a consequence of the drastic change in the germanium structure. The CRIME technique makes it possible to choose an implantation material which is less sensitive to radiation damage.

Figure 5 shows four Mössbauer spectra, all observed with the same crystalline Ge absorber (138-mg/cm^2 natural germanium at 78°K) but with different host materials for the targets, Ge, Cu, Fe, and Cr. Every spectrum contains about 180 data points with an error of a few times 10^{-3} per datum. All spectra could be fitted with a Lorentzian curve. A least-squares fit to the data yields the height, the half-width, and the position of the absorption line. These values were used in the analysis of our data. Taking into account the uncertainties of these three parameters, the observed spectra are plotted as envelopes to avoid the confusion due to 720 data points in one figure. As can be seen, the Mössbauer effect is considerably increased over that observed with a thick germanium target when Cu, Fe, or Cr is used as the implantation host. The largest effect was observed when ^{73}Ge was implanted into chromium, and therefore most of our investigations were performed with a germanium on chromium target.

For these targets our experiments indicate a line broadening, but only for targets which were not exposed to more than about 100-μA h of integrated oxygen beam. After sufficient irradiation the line narrows to its natural width and remains that way for extended periods of irradiation. We assume that the line broadening in undamaged Ge on Cr targets can be explained by magnetic hyperfine fields acting on the ^{73}Ge nuclei in antiferromagnetic chromium. The observed narrowing of the linewidth would then indicate destruction of the magnetic order due to radiation damage.

Neutron diffraction experiments with pure chromium indicated the existence of spin-density waves[39] below 311°K. Recent Mössbauer experiments with ^{119}Sn as an impurity in Cr yielded broadened spectra.[40] This result was explained on the basis of a linear spin-density wave model.[41] The model predicts a distribution of internal magnetic fields with the distribution function

$$w(H)dH=[2/\pi(H_0^2-H^2)^{1/2}]dH, \quad \text{for} \quad 0\leq H\leq H_0$$
$$=0, \quad \text{otherwise.} \qquad (23)$$

We will use the same model in the analysis of the observed line broadening for ^{73}Ge and combine this with the approximation introduced in Sec. III B. Since Δ is proportional to H, the distribution function of Δ is given also by

$$W(\Delta)d\Delta=[2/\pi(\Delta_0^2-\Delta^2)^{1/2}]d\Delta \quad \text{for} \quad 0\leq\Delta\leq\Delta_0, \qquad (24)$$

where

$$\Delta_0\equiv 2H_0\,|\,\mu_e-\mu_g\,|\,\tau_n/\hbar.$$

If we assume that all initial magnetic substates are equally populated,[42] and that the internal field directions are randomly distributed, the frequency distribution function Eq. (19) is modified to

$$D(\delta\omega)=\frac{\tau_n}{\pi\Delta_0}\ln\left\{\frac{1+[1-(2\tau_n\delta\omega/\Delta_0)^2]^{1/2}}{1-[1-(2\tau_n\delta\omega/\Delta_0)^2]^{1/2}}\right\},$$
$$\text{for} \quad |\,\delta\omega\,|\leq\Delta_0/2\tau_n$$
$$=0, \quad \text{otherwise.} \qquad (25)$$

The logarithmic singularity at $\delta\omega=0$ vanishes, if Eq. (25) is folded into the natural Lorentzian line shape, which must be done in order to get the recoilless emission spectrum of the source,

$$I(\omega)\propto\int_{-\Delta_0/2\tau_n}^{\Delta_0/2\tau_n}\frac{D(\delta\omega)}{(\omega-\omega_0-\delta\omega)^2+(\Gamma/2\hbar)^2}\,d(\delta\omega). \qquad (26)$$

For a broadening parameter Δ_0 between 0.5 and 2 the spectrum $I(\omega)$ resembles a broadened Lorentzian with a full width at half-maximum of $\Gamma(1+2\gamma)$, where

$$\gamma\approx\frac{\frac{1}{2}\Delta_0}{1+\ln(2\Delta_0)}, \qquad 0.5\lesssim\Delta_0\lesssim 2.$$

The parameters of the observed Mössbauer line are

[39] R. Street and B. Window, Proc. Phys. Soc. (London) **89**, 587 (1966).
[40] T. J. Bastow and R. Street, Phys. Rev. **141**, 510 (1966).
[41] A. W. Overhouser, J. Phys. Chem. Solids **13**, 71 (1960); Phys. Rev. **128**, 1437 (1962).
[42] For our experimental conditions this assumption is quite good; however, an experiment which does demonstrate the inequality was performed by S. S. Hanna, G. D. Sprouse, and G. M. Kalvius, in *Proceedings of the International Conference on Hyperfine Interactions Detected by Nuclear Radiation, Asilomar, 1967* (North-Holland Publishing Co., Amsterdam, 1968).

obtained after a final folding of $I(\omega)$ with the exponential attenuation function for an absorber with an unsplit absorption line. From our observed Mössbauer spectra with germanium on chromium sources we deduce

$$\gamma=0.37\pm0.12, \quad \text{yielding} \quad \Delta_0\approx1.6\pm0.8.$$

As will be shown in Sec. IV D, the Δ parameter of Ge in Fe is approximately the same.

It should, however, be noted that we have not considered other mechanisms of line broadening such as quadrupole splitting. Such effects cannot be excluded by the data, and their presence would modify the analysis.

B. Temperature Dependence of Crystalline Germanium Absorbers and the Excited State Spin

The Mössbauer spectra taken with radiation-damaged Cr:Ge-implantation[43] sources and thin crystalline germanium absorbers show a width which extrapolates to the natural linewidth at zero absorber thickness, full width at half-maximum, $2v_{1/2}=(2.2\pm0.1)$ mm/sec yielding a mean life $\tau_n=(2.68\pm0.14)$ nsec. This value is not inconsistent with the electronically measured mean lifetime[44] (2.33 ± 0.20) nsec of the excited state.

In a first series of measurements we have taken Mössbauer spectra at 78°K with absorbers of different thicknesses.[16] For a single-line absorber, the maximum effect $M(0)$, the observed width at half-maximum $V_{1/2}$, and the area F, under the Mössbauer line are well-known functions of the effective absorber thickness corresponding to the curves in Fig. 4 designated by $\Delta=0$.

The spin j_e of the 67.03-keV state was thought to be either $\frac{7}{2}$ or $\frac{1}{2}$. However, T_{eff} defined in Eq. (22) is spin-dependent:

$$T_{\text{eff}}=n_a\sigma_0 f_a$$
$$=[2\pi n_a\lambda\!\!\!^{-2}f_a/(1+\alpha_{ic})](2j_e+1)/(2j_g+1). \quad (27)$$

According to Fig. 4, T_{eff} is obtainable from the observed Mössbauer spectrum. The recoilless fraction f_a of the absorber is directly related to thermodynamic data[45] or to the phonon spectrum of germanium.[46] Therefore, f_a as well as n_a, $\lambda\!\!\!^{-}$, α_{ic}, and j_g are known quantities in Eq. (27) and the unknown spin j_e can be determined in principle. However, due to the number of parameters involved and the additional uncertainty caused by the radiation-induced transitions in the targets, it was not advisable to rely on a single measurement to determine the excited state spin. If the implantation technique is used, the apparent recoilless fraction of the source

$$f_s=\eta f_s\,(\text{Cr:Ge})+(1-\eta)f_s\,(\text{Ge:Ge}) \quad (28)$$

depends upon the implantation ratio η and the Debye-Waller factors of Ge implanted into Cr and into Ge, respectively. For our targets the second term is at least 20 times smaller than the first one and will be neglected. With the aid of the $\Delta=0$ curves in Fig. 4 the single-line Mössbauer spectra yield values for T_{eff} and f_s. When the spin factor in Eq. (27), and the implantation ratio in Eq. (28) are not known, we can only deduce the products ηf_s (Cr:Ge) and $[(2j_e+1)/(2j_g+1)]f_a$.[47] The data taken with Cr:Ge target No. 1 gave

$$[(2j_e+1)/(2j_g+1)]f_a\,(\text{Ge, }78°\text{K})=(4.57\pm0.38)\%,$$
$$(\eta f_s)_1=(5.40\pm0.38)\%. \quad (29)$$

For any other target, for example No. 2, the value $(\eta f_s)_2$ was determined by relating the areas F under two Mössbauer spectra taken with identical absorbers:

$$(\eta f_s)_2/(\eta f_s)_1=F_2/F_1. \quad (30)$$

Equation (30) is correct even if the emission spectrum of source No. 2 is broadened.

The phonon spectrum $g(\Omega)$ of germanium is known,[46] and consequently $f\,(\text{Ge}, T)$ can be calculated. In order to test the calculated temperature dependence of $f\,(\text{Ge}, T)$ and, simultaneously, to determine the spin factor $(2j_e+1)/(2j_g+1)$, we have measured the recoilless fraction of a Ge-absorber for $78°\leq T_{\text{abs}}\leq221°$K. The undamaged Cr:Ge-implantation source (Source No. 2) was held at liquid-nitrogen temperature, and data were taken alternatively at zero velocity and with a large vibrator amplitude ($v_{\max}\gg V_{1/2}$). The data analysis was then performed by the approximate method described in Sec. III B. The characteristic source parameters were $(\eta f_s)_2=(4.43\pm0.34)\%$ and $\gamma=0.37\pm0.12$. In Fig. 6 the logarithm of the deduced values $f\,(\text{Ge}, T)(2j_e+1)/(2j_g+1)$ is plotted versus temperature. The error bars are not purely statistical as they include the uncertainties in $(\eta f_s)_2$ and γ.

The Debye-Waller factor in the high-temperature approximation is given by[48]

$$-\ln f=\langle x_0^2\rangle_T/\lambda\!\!\!^{-2}$$
$$=\frac{1}{\lambda\!\!\!^{-2}}\frac{1}{M_0}\left(\langle\Omega^{-2}\rangle_g kT+\frac{\hbar^2}{12kT}-\frac{\hbar^4\langle\Omega^2\rangle_g}{720(kT)^3}\right.$$
$$\left.+\frac{\hbar^6\langle\Omega^4\rangle_g}{30\,240(kT)^5}-\frac{\hbar^8\langle\Omega^6\rangle_g}{1\,209\,600(kT)^7}+\cdots\right), \quad (31)$$

where the frequency moments are defined by

$$\langle\Omega^n\rangle_g\equiv\int\Omega^n g(\Omega)\,d\Omega. \quad (32)$$

[43] Where the notation Cr:Ge or Ge:Ge indicates that Ge is implanted into Cr, or into Ge, respectively.

[44] R. E. Holland and F. J. Lynch, Phys. Rev. **121**, 1464 (1961).

[45] L. S. Salter, Advan. Phys. **14**, 1 (1965).

[46] G. Dolling and R. A. Cowley, Proc. Phys. Soc. (London) **88**, 463 (1966).

[47] In Ref. 16 we have derived a value for the recoilless fraction of Ge in Ge from these data. However, in the analysis we assumed $j_e=11/2$, and we had at that time no evidence for the line narrowing in irradiated targets. In view of new experiments we have now reevaluated the data applying a method which eliminates the effects of line broadening.

[48] J. Petzold, Z. Physik **163**, 71 (1961).

TABLE II. Properties of germanium in chromium.

T(°K)	$F/(\eta f_a)_{2\pi v_{1/2}}$	$-\ln f$	q (10^{-5} cm²/erg)	q_0 (10^{-5} cm²/erg)	q/q_0
78	1.24±0.15	1.78±0.19	0.77±0.15	0.560	1.38±0.26
105	0.98±0.12	2.20±0.24	0.96±0.14	0.710	1.35±0.19
130	0.72±0.09	2.64±0.14	1.03±0.07	0.745	1.38±0.10
160	0.58±0.07	2.98±0.20	1.01±0.08	0.760	1.33±0.10

The frequency moments for germanium have been deduced by Dolling and Cowley[46] from phonon dispersion relations obtained from inelastic neutron scattering, whereas Salter[45] determined the moments directly from the temperature dependence of thermodynamic data. Both procedures lead to nearly equal results, except for $\langle\Omega^{-2}\rangle_g$, for which Dolling obtains 2.20×10^{-27} sec² and Salter $(2.00\pm0.05)\times10^{-27}$ sec². Anharmonic effects, which were not properly taken into account in either treatment, may be partly responsible for this discrepancy.

Since the quantities $\langle\Omega^n\rangle_g$ are known, values for the spin j_e may be assumed in order to calculate

$$-\ln[f(2j_e+1)/(2j_g+1)]=$$
$$-\ln f-\ln\{(2j_e+1)/(2j_g+1)\}$$

for comparison with the data of Fig. 6. The Coulomb-excitation data have limited j_e to the value $\frac{7}{2}$ or $\frac{11}{2}$.[22] With these spin values and $j_g=\frac{9}{2}$ we obtain the two shaded areas in Fig. 6. It is clear that $j_e=\frac{7}{2}$ gives a much better fit to the data than does $j_e=\frac{11}{2}$. Within the investigated temperature region $78°K\leq T\leq221°K$ the observed Debye-Waller factor is then in agreement with the solid-state properties of germanium provided the spin of the 67.03-keV state is $j_e=\frac{7}{2}$. This value is used in all subsequent data evaluations. The recoilless fraction of germanium at 78°K is then according to Eq. (29):

$$f_a\,(\mathrm{Ge},\,78°K)=(5.72\pm0.47)\,\%.$$

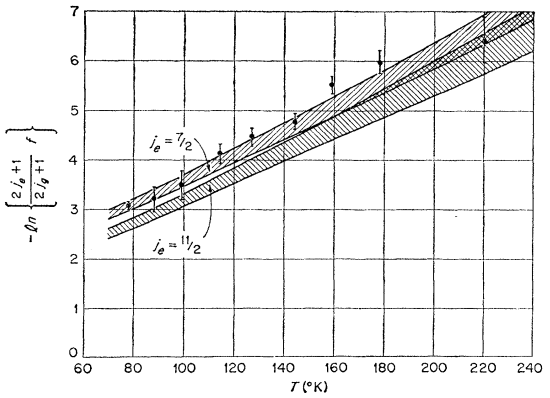

FIG. 6. The data points are the measured recoilless fractions of a crystalline germanium absorber (276-mg/cm² natural Ge) as a function of temperature. The upper and lower bands were calculated assuming a nuclear excited state spin of 7/2 and 11/2, respectively, with the frequency moments derived from neutron scattering data (upper boundary), and from thermodynamic data (lower boundary) (see Refs. 46 and 45, respectively). The breadths of the bands represent the uncertainties in the knowledge of the phonon spectrum for germanium. The data are consistent with $j_e=7/2$.

C. Germanium as an Impurity in Chromium and the Recoilless Fraction in Other Implantation Targets

An absorber which contained a 1.76% atomic abundance of Ge in chromium equivalent to 10.4 mg/cm² of ^{73}Ge was used to investigate the following: (1) line broadening, as seen in undamaged Cr:Ge targets, (2) radiation damage by comparison of the f factor for the Cr:Ge implantation targets with that of the Ge(Cr) absorber, and (3) the validity of the impurity model of Sec. III A.

Four Mössbauer spectra were taken, at absorber temperatures of 78, 105, 130, and 160°K. At 130 and 160°K we observed the natural linewidth (after an appropriate correction for finite absorber thickness), indicating that neither the emission spectrum (due to a radiation damaged Cr:Ge source) nor the absorber line were broadened. Although the spectra measured earlier at 78 and 105°K showed a slight broadening, we could not determine whether the source or the absorber was broadened because the magnetic state of the source was unknown. Hyperfine splitting at low temperature might be expected because spin-density waves[40] occur in pure chromium below 311°K. Of course, the Ge content of the alloy may be sufficient to reduce the Néel temperature below our working temperature.

In order to compare the observed recoilless fraction for 1.76% germanium in chromium with the prediction of the impurity model, the q value, defined in Eq. (10), has to be determined. The results of the analysis are given in Table II. The second column contains the normalized area under the observed Mössbauer absorption curve. To obtain the values of $-\ln f$ given in the third column, Fig. 4(c) was used to relate the area F and the effective absorber thickness T_{eff}, which is proportional to f.[49] The expression for q can be written as

$$q=\frac{-\lambda^2\ln f-\hbar^2/(12MkT)}{kT}. \qquad (33)$$

[49] If Fig. 4(c) is used, Δ has to be known. For $T\geq130°K$ no broadening occurred, i.e., $\Delta=0$. For $T=78$ and 105°K we allow $0\leq\Delta\leq1.5$.

Therefore, q follows directly from $-\ln f$ and is listed in column four of Table II. Because the phonon spectrum $g(\Omega)$ for chromium is available, q_0, defined in Eq. (12), can be calculated:

$$q_0=\left\{\frac{\hbar}{M_0}\int_0^\infty\frac{g(\Omega)}{\Omega}\left[\frac{1}{2}+\left(\exp\left(\frac{\hbar\Omega}{kT}\right)-1\right)^{-1}\right]d\Omega-\frac{\hbar^2}{12M_0kT}\right\}\Big/kT. \tag{34}$$

The values of q_0 and q/q_0 as a function of temperature are listed in the last two columns of Table II. In agreement with Eq. (12) the ratio is temperature-independent.

For the bcc structure of chromium, Eq. (12) becomes

$$q/q_0=1+0.63(\alpha_0-\alpha)/\alpha, \tag{35}$$

and from the weighted average $q/q_0=1.36\pm0.06$ we obtain $\alpha/\alpha_0=0.64\pm0.04$. The spring constant of the Ge–Cr pair is therefore approximately $\frac{2}{3}$ of the Cr–Cr spring constant.

The f factor of the Ge(Cr) absorber may be compared with the recoilless fractions of the Cr:Ge-implantation targets. As discussed in Sec. IV B, measurements with the first Cr:Ge target yielded the value $(\eta f_s)_1=(5.40\pm0.38)\%$. Assuming an implantation ratio $\eta=0.65\pm0.1$ (compare Table I) we get $f_s\,(\mathrm{Cr:Ge})=(8.3\pm1.5)\%$. On the other hand, for the temperature of 78°K, which was the temperature of the target, Table II indicates the absorber recoilless fraction is $f_a[1.76\%\ \mathrm{Ge(Cr)}]=(17\pm3)\%$. The reduction in the recoilless fraction of the target is probably due to radiation damage.

The impurity model furnishes a very simple description of how radiation damage may change the Mössbauer effect. At the end of the slowing down process of the Coulomb-excited atom, many displacement collisions occur. Therefore the impurity may stop in the neighborhood of vacancies.[27–29] The cage, normally constituted of the n nearest neighbors, now possesses Δn holes. Every time the Mössbauer atom approaches a vacancy, which occurs for a fraction $\Delta n/n$ of all interior vibrations, it will travel farther than it would in the undamaged cage. Typical vibration amplitudes in the latter case are 10^{-9} cm, mainly limited by the repulsive core of the interatomic forces between the atoms. But for vibrations in the direction of a vacancy the absence of a repulsive core may cause an increase in the amplitude by a factor p of about 2 or 3, depending upon the interatomic forces. The contribution of the motion inside a radiation damaged cage to the mean square vibration amplitude $\langle x^2\rangle_T$ is therefore $[p^2\Delta n+(n-\Delta n)]/n$ times larger than in the corresponding undamaged cage. According to Eq. (9), at high temperature the impurity atom in an undamaged cage contributes to $\langle x^2\rangle_T$ only by the term $(A/\alpha)kT$. This consideration shows that radiation damage affects the impurity-model equations simply by replacing the impurity spring constant α by an effective constant[50]

$$\alpha_{\mathrm{eff}}=\alpha[(p^2-1)(\Delta n/n)+1]^{-1}. \tag{36}$$

[50] The low-frequency phonon spectrum, represented in Eq. (9) by $(B/\alpha_0)kT$, is assumed to be insensitive to radiation damage.

From the Debye-Waller factor $f_s\,(\mathrm{Cr:Ge})=(8.3\pm1.5)\%$ and Eqs. (33) through (35), we obtain $\alpha_{\mathrm{eff}}/\alpha_0=0.32\pm0.04$ (see Table III). Inserting this value and the value $\alpha/\alpha_0=0.64\pm0.04$ of the undamaged absorber spring constant into Eq. (36) yields $(p^2-1)\Delta n/n=1\pm0.3$. A reasonable choice for Δn and p of approximately 2 would explain this result. Of course, the real processes are much too complicated to be represented by a simple formula such as Eq. (36), and the results of the above analysis are therefore only qualitative.

In addition to the Cr:Ge target we have tried copper and iron as an implantation material. In order to obtain the Debye-Waller factors the areas under the curves were determined and compared with the area under the corresponding spectrum of the first Cr:Ge target for which $f\,(\mathrm{Cr:Ge})=(8.3\pm1.5)\%$. Provided that the implantation ratios η are approximately the same for all our targets, Eq. (30) shows that the ratio of the areas directly gives the ratio of the recoilless fractions. Since the actual target thickness, and hence η, is not well known, we have included this uncertainty in the error bars. The results are listed as $-\ln f$ (78°K) in the third column of Table III. In the last three columns a comparison is made with the radiation-damaged impurity model. To obtain q_0 for iron or copper, Eq. (12), (34), or (31) was used. The phonon spectrum of iron, needed in Eq. (34), is known from neutron scattering experiments.[51] For copper the frequency moments $\langle\Omega^n\rangle_a$ needed in Eq. (31) were deduced from thermodynamic data (Salter, Ref. 45).

D. Magnetic Line Broadening in the Fe_5Ge_3 Absorber

An Fe_5Ge_3 absorber was used to search for a magnetic hyperfine interaction. Fe_5Ge_3 has a structure belonging to the symmetry group $B8_2(Ni_2In)$,[52] and is ferromagnetic. Mössbauer studies with ^{57}Fe have proved the existence of three different magnetic iron sites with internal fields of 136, 214, and 256 kG, respectively.[53] It may be expected, that the 4s electrons on the germanium atoms become partly polarized through an exchange interaction with their nearest iron neighbors. This will lead to a hyperfine field H acting on the Ge nucleus,[54] and an observable line broadening may result.

Our Fe_5Ge_3 absorber contained 10.9 mg/cm^2 of ^{73}Ge. A Mössbauer spectrum was taken at $T=78$°K, using the radiation damaged Cr:Ge target and is shown in Fig. 7. The observed spectrum was fitted with a Lorent-

[51] W. Gläser (private communication).
[52] G. S. Barrett, *Structure of Metals* (McGraw-Hill Book Co., New York, 1952), 2nd ed.
[53] H. Yamamoto, J. Phys. Soc. Japan **20**, 2166 (1965).
[54] For Sn in metallic iron, $H=80$ kG, A. J. F. Boyle, D. St. P. Bunberry, and C. Edwards, Phys. Rev. Letters **5**, 553 (1960).

TABLE III. Comparison of effective spring constants for Ge implanted into Cr, Fe, and Cu.

Target	Structure	$-\ln f$ (78°K)	q (10^{-5} cm²/erg)	q_0 (10^{-5} cm²/erg)	$\alpha_{\text{eff}}/\alpha_0$
Cr:Ge	bcc	2.48±0.19	1.33±0.15	0.56	0.32±0.04
Fe:Ge	bcc	3.3 ±0.4	2.0 ±0.3	0.81	0.3 ±0.1
Cu:Ge	fcc	3.8 ±0.4	2.4 ±0.3	1.55	0.6 ±0.1

zian, and a least-squares fit to the data yielded the solid curve shown in the figure with the following parameters: (1) isomer shift $\delta=0.06\pm0.06$ mm/sec; (2) maximum effect $M(0)/(\eta f_s)_2=0.49\pm0.04$; (3) relative broadening, $V_{1/2}/v_{1/2}=1.48\pm0.11$; and (4) area under the absorption line, $F/[\pi v_{1/2}(\eta f_s)_2]=0.727\pm0.065$. A crystalline Ge absorber with the same source gave an unbroadened line located at $\delta=0.02\pm0.06$ mm/sec. The absence of any noticeable isomer shift between Fe_5Ge_3 and Ge indicates that the number of 4s electrons at the Ge nucleus is about the same in both crystals (approximately one, see Sec. IV E).

The Fe_5Ge_3 absorption line was somewhat broader than the line of the pure Ge absorber with a comparable effective thickness. This line broadening is probably caused by a magnetic hyperfine interaction, although a distribution of isomer shifts cannot be excluded. For this case the Δ approximation of Sec. III B applies. The broadening parameter Δ and the effective absorber thickness T_{eff} are unknown and can be determined as demonstrated in Fig. 8 using Fig. 4. For example, the observed linewidth $V_{1/2}/v_{1/2}=1.48\pm0.11$ defines a band in Fig. 4(b) parallel to the abscissa. This band is mapped onto the (T_{eff}, Δ) plane, displayed in Fig. 8. The same procedure applied to $M(0)/(\eta f_s)$ and $F/(\eta f_s \pi v_{1/2})$ determines three regions of the (T_{eff}, Δ) plane. Their common intersection contains the most likely (T_{eff}, Δ) pair, $T_{\text{eff}}=1.95\pm0.15$ and $\Delta=1.6\pm0.3$. Inserting these numbers into Eqs. (22) and (16) we obtain $f(Fe_5Ge_3;\ 78°K)=(6.1\pm0.5)\%$ and $H\,|\,\mu_e-\mu_g\,|=(125\pm25)\mu_N$ kG.

A Δ parameter may also be deduced from the Fe:Ge implantation spectrum shown in Fig. 5. Although all four spectra in this figure were taken with the same absorber, the Fe:Ge line is somewhat broadened. In order to explain the broadening in terms of the Δ approximation, $\Delta=1.7\pm0.7$ has to be assumed. The magnetic hyperfine fields acting on a Ge nucleus in Fe or Fe_5Ge_3 are about equal.

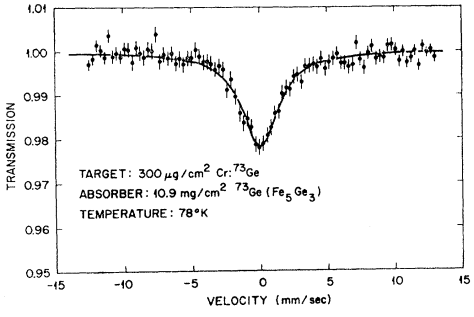

FIG. 7. Mössbauer spectrum of an Fe_5Ge_3 absorber with a Cr:Ge target. The width of the absorption line is indicative of a magnetic hyperfine interaction with the ^{73}Ge nuclei.

E. Isomer Shift and Recoilless Fraction of GeO_2

The isomer shifts observed in Mössbauer spectra provide information about nuclear and chemical properties. They are most clearly observed between compounds corresponding to different valence states. As GeO_2 is the most convenient ionic compound of Ge available, it was chosen to investigate any isomer shift relative to germanium that might occur.

Two forms of germanium dioxide are known to exist. The dense, water-insoluble form has a rutile structure with a tetragonal unit cell, and the second form has the trigonal quartz structure with a hexagonal unit cell.[55] The Mössbauer spectra for these two forms are displayed for comparison in Fig. 9. Both absorbers con-

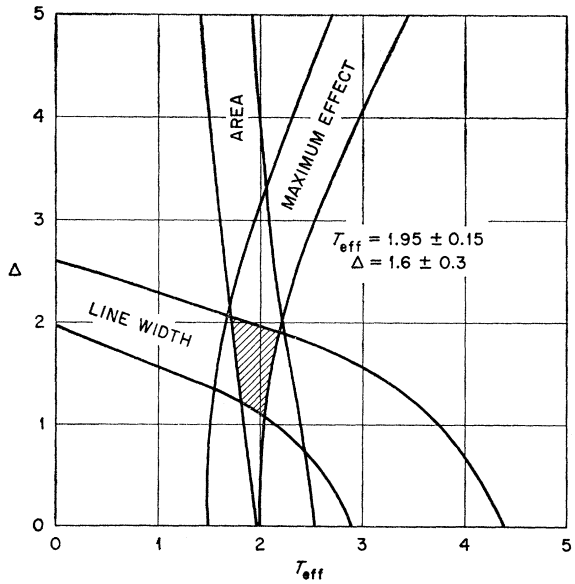

FIG. 8. With information obtained from Figs. 4 and 7, a value for the broadening parameter Δ and the effective thickness T_{eff} may be determined for the Fe_5Ge_3 absorber. The procedure is illustrated in the figure.

[55] R. W. Wyckoff, *Crystal Structures* (Interscience Publishers, Inc., New York, 1948).

TABLE IV. Recoilless fractions and isomer shifts of GeO_2.

Compound	Density (g/cm^3)	Coordination number of Ge ion	Recoilless fraction f (%)	Isomer shift (relative to Ge) mm/sec
GeO_2 (hex)	4.228	4	6.1±0.7	−(1.0±0.10)
GeO_2 (tetr)	6.238	6	32±5	−(0.96±0.18)

tained 10.71 mg/cm² of ^{73}Ge as powdered GeO_2, while the Cr:Ge target No. 2 was used. Neither spectra show any conclusive evidence for magnetic dipole or electric quadrupole broadening. Therefore, Fig. 4 with $\Delta=0$ can be used to obtain the recoilless fractions f. The results are listed in Table IV, together with the densities and oxygen coordination numbers for the two forms of GeO_2. The last column of the table gives the observed isomer shift with respect to crystalline Ge.

As may be seen from Table IV, the recoilless fraction for GeO_2 (tetr) is larger by a factor of about 5 than for GeO_2 (hex). This difference may be due to the fact that the dense, close packed lattice of GeO_2 (tetr) results in an increased number of oxygen near neighbors (six) for the Ge^{4+} ion. An increased recoilless fraction with increased coordination number was first observed for ^{119}Sn compounds.[56]

Both absorbers show about the same isomer shift relative to Ge. An isomer shift δ is observed when the chemical environment of the nucleus is different in source and absorber. δ is given by

$$\delta=\tfrac{4}{5}\pi Ze^2R^2(\Delta R/R)[\rho_{\rm abs}(0)-\rho_{\rm source}(0)], \quad (37)$$

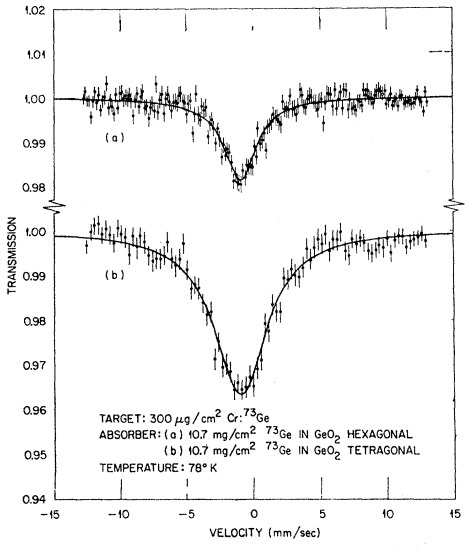

FIG. 9. The Mössbauer spectra shown were measured for the two different modifications of GeO_2: (a) hexagonal and (b) tetragonal. See Table IV for the information which may be derived from these spectra.

[56] V. I. Gol'danskii, E. F. Makarov, R. H. Stukan, T. N. Sumarova, V. A. Truktanov, and V. V. Khrapov, Dokl. Akad. Nauk SSSR **156**, 400 (1964).

where R is the charge radius of the nucleus, ΔR the difference between this quantity for the excited and ground states, and $e\rho(0)$ the total electronic charge density at the nucleus. In order to derive a value of $\Delta R/R$ for the Mössbauer nucleus from the observed isomer shifts, one must estimate $\rho(0)$ for the electronic configurations corresponding to the materials used. We have interpreted our isomer-shift data by calculating electron wave functions for various electronic configurations using the computer code RELWAV-WSX.[57] Features of the calculation are as follows: (1) The Dirac equation is used to compute the one-electron orbitals. (2) The many-electron wave function is then obtained using the Hartree variational technique including an average exchange potential (Slater-Latter approximation). (3) The effect of the solid on the wave functions is taken into account by imposing boundary conditions on the radial wave functions at the Wigner-Seitz radius. (4) A finite-sized nucleus was considered with a Fermi charge distribution.

Calculations were made for the following electronic structures: $Ge(4s^14p^3)$, $Ge(4s^24p^2)$, $Ge^{2+}(4s^24p^0)$, $Ge^{2+}(4s^14p^1)$, and $Ge^{4+}(4s^04p^0)$, and in each case for several values of the Wigner-Seitz radius r_0. The results for the electron densities are listed in Table V.

Although the degree of covalency of the Ge^{4+} ions in GeO_2 is not known, we assume the configuration $Ge^{4+}(4s^04p^0)$ in this case. For crystalline Ge the appropriate configuration is $Ge(4s^14p^3)$.[58] Values for the total electronic charge density at the nucleus for both cases are given in Table V. The difference in charge density is quite sensitive to the choice of the Wigner-Seitz radius r_0. The value of r_0, 1.22×10^{-8} cm for pure germanium is half of the Ge–Ge distance. We adopt this value for Ge as well as for GeO_2 and obtain from Table V the appropriate difference in electronic densities: $\rho(4s^04p^0)-\rho(4s^14p^3)=-0.75\times10^{26}$ electrons/cm³. Due to the relativistic procedure of RELWAV-WSX no relativistic corrections are needed in Eq. (37). With the calculated electron density difference and a nuclear

[57] C. W. Nestor, T. C. Tucker, T. A. Carlson, L. D. Roberts, F. B. Malik, and C. Froese, Oak Ridge National Laboratory Report No. ORNL-4027, 1966 (unpublished).

[58] There is now evidence that the configurations, which were used in these calculations, are correct. For Ge^{2+} the configuration $4s^24p^0$ is expected. This would result in a positive isomer shift between Ge^{2+} and Ge^{4+} of about 2.9 mm/sec. A shift of this magnitude was recently observed at Erlangen. This experimental result was (2.3±0.4) mm/sec. B. Zimmermann, H. Jena, G. Ischenko, H. Kilian, and D. Seyboth, Phys. Status Solidi **27**, 639 (1968).

TABLE V. Total relativistic electron density at the nucleus.

Configuration	Wigner-Seitz radius r_0 (Å)	Electronic density $\rho(0)$ (10^{26} cm^{-3})
$4s^14p^3$	1.01	2129.871
	1.19	2129.300
	1.32	2129.062
	1.40	2128.971
	1.59	2128.864
	1.80	2128.859
	1.85	2128.872
	2.80	2129.296
$4s^24p^2$	1.32	2130.104
	1.59	2129.682
	1.85	2129.670
$4s^24p^0$	1.32	2130.598
	1.59	2130.294
	1.85	2130.451
$4s^14p^1$	1.32	2129.391
	1.59	2129.219
	1.85	2129.307
$4s^04p^0$	1.32	2128.396
	1.59	2128.313
	1.85	2128.296

charge radius $R=5.23\times10^{-13}$ cm as given by Elton,[59] Eq. (37) can be written in terms of velocity units:

$$\delta=-(106\text{ cm/sec})\Delta R/R. \tag{38}$$

The observed isomer shift for the two GeO_2 absorbers are equal within the quoted error bars (Table IV). From the average value $\delta=-(0.98\pm0.07)$ mm/sec and Eq. (38) we obtain $\Delta R/R=+0.9\times10^{-3}$. We estimate that the uncertainty in $\Delta R/R$ is about 30%. In the following section the experimental $\Delta R/R$ value is compared with nuclear models.

V. NUCLEAR PROPERTIES OF ^{73}Ge

The nuclear properties of ^{73}Ge deduced in the present Mössbauer studies, may be compared with those predicted by various nuclear models. Few calculations exist for ^{73}Ge as this nucleus is not expected to be well described by the shell model, and even the even-even germanium nuclei have poorly understood level schemes. Nevertheless, the single-particle core-coupling model may be used to attempt to understand the properties of odd-A nuclei[60,61] such as ^{73}Ge. In this model, the nucleus is considered as an odd particle weakly coupled to an even-even core. The ground-state spin should then equal the angular momentum of the odd particle. Collective oscillations of the core can be excited as they are in the neighboring even-even nuclei, but are split into a number of levels by the single-particle core coupling.

In the simple single-particle core-excitation model, the low-lying levels of ^{73}Ge are considered to be multiplets arising from the coupling of the $1g_{9/2}$ particle to the even-even core states, which should be similar to those for the neighboring even-even nuclei such as ^{72}Ge and ^{74}Ge. This would then give a ground-state spin of $\frac{9}{2}^+$ consistent with the known value for ^{73}Ge. Similarly, coupling the $1g_{9/2}$ particle to the first 2^+ state of the core produces a quintet of states with spins $\frac{5}{2}^+$, $\frac{7}{2}^+$, $\frac{9}{2}^+$, $\frac{11}{2}^+$, and $\frac{13}{2}^+$. While this interpretation would be consistent with the spin of $\frac{7}{2}$ assigned to the 67.03-keV state as discussed in Sec. VI B, the high spin values being coupled do not make the core-excitation model very selective in this case. In addition, the probable $\frac{5}{2}^+$ state at 13.5 keV is the only other state known in ^{73}Ge with the proper spin to be a member of a quintet based on a 2^+ core state.

Properties of ^{73}Ge have also been calculated using the pairing plus quadrupole model.[62,63] In this model the nuclear system is treated as a core plus a few valence particles. The valence particles interact independently with the core, and with each other through two-body forces. In particular, the ^{73}Ge calculations of Uher[64] considered quasiparticles with spins of $\frac{5}{2}$, $\frac{7}{2}$, and $\frac{9}{2}$ coupled to a zero-phonon, 0^+ state and a one-phonon, 2^+ state. For ^{73}Ge this model then predicts a $\frac{9}{2}^+$ ground state and a low-lying $\frac{7}{2}^+$ excited state, with a value for $\Delta R/R$ for the $\frac{7}{2}^+$ to $\frac{9}{2}^+$ transition of $+1.37\times10^{-3}$. This prediction is in reasonable agreement with the measured value of $(0.9\pm0.3)\times10^{-3}$ (see Sec. IV E).

A further test of this model may be obtained by comparing the calculated and measured $B(E2)$ values for the transition between the $\frac{9}{2}^+$ and $\frac{7}{2}^+$ states. The form for the reduced $E2$ transition probability in the pairing plus quadrupole model for an odd-A nucleus has been given by Sorensen.[65] Using the wave functions calculated by Uher[64] and a $B(E2)$ value of 2.68×10^{-49} e^2 cm^4, the average of the values[66] for ^{72}Ge and ^{74}Ge, for the reduced $E2$ transition rate for exciting the first excited state of the core, a $B(E2)$ value of 0.28×10^{-49} e^2 cm^4 was obtained for the $\frac{9}{2}^+\rightarrow\frac{7}{2}^+$ transition in ^{73}Ge. While the experimental value is 0.57×10^{-49} e^2 cm^4,[22] the difference of a factor of 2 is not unusual in comparing calculated and experimental results.[65] Part of the difficulty may arise from using an average of the experimental $B(E2)$ values for the $0^+\rightarrow2^+$ transition in the neighboring even-even nuclei for the core transition

[59] L. R. B. Elton, *Nuclear Sizes* (Oxford University Press, Oxford, 1961), see Eq. (2.80), p. 56.
[60] R. D. Lawson and J. L. Uretsky, Phys. Rev. **108**, 1300 (1957).
[61] A. de-Shalit, Phys. Rev. **122**, 1530 (1961); Phys. Letters **15**, 170 (1965).
[62] L. S. Kisslinger and R. A. Sorensen, Rev. Mod. Phys. **35**, 853 (1963).
[63] R. A. Uher and R. A. Sorensen, Nucl. Phys. **86**, 1 (1966).
[64] R. A. Uher (private communication).
[65] R. A. Sorensen, Phys. Rev. **133**, B281 (1964).
[66] P. H. Stelson and L. Grodzins, Nucl. Data **1**, 21 (1965).

rate. The core of ^{73}Ge may differ considerably from the even-even nuclei ^{72}Ge and ^{74}Ge. In addition, the general core-excitation model of de-Shalit[61] predicts that the reduced $E2$ transition probabilities for decay from the members of the multiplet based on the 2^+ state of the core will be equal to that between the 2^+ and 0^+ states in the adjacent even-even nuclei. As the $B(E2)$'s for decay for ^{72}Ge and ^{74}Ge are 0.44×10^{-49} e^2 cm^4 and 0.63×10^{-49} e^2 cm^4, respectively,[66] only the value for ^{74}Ge is approximately equal to the ^{73}Ge de-excitation $B(E2)$, 0.72×10^{-49} e^2 cm^4. However, even if a value of 0.72×10^{-49} e^2 cm^4 is adopted for the core as predicted by the core-excitation model, the pairing plus quadrupole result is still only 0.37×10^{-49} e^2 cm^4.

If the broadening of the Fe_5Ge_3 absorption line is assumed to be due to simple magnetic splitting, then the data are compatible with a value for the product $H_{\text{eff}}|\mu_e-\mu_g|$ of approximately 125 μ_N kG (see Sec. IV D). This does not yield a value for the internal magnetic field, since a calculation of the magnetic moment of the $\frac{7}{2}^+$ excited state is not presently available, even though the pairing plus quadrupole model gives general agreement between the calculated and measured isomer shifts and $B(E2)$'s, due to the difficulty in including the effects of currents in the core.

VI. SUMMARY

The Mössbauer effect has been studied following the implantation of Coulomb-excited ^{73}Ge nuclei into various host materials. This method furnishes a technique for obtaining information concerning germanium and germanium as an impurity atom which cannot otherwise be obtained.

Simplified models describing impurities in solids and magnetic line broadening were developed for analyzing the experimental data. These models provide a useful picture of the physical processes involved, and a means with which the significant parameters of the theory could be easily computed.

Solid-state properties of germanium as an impurity in different host materials were obtained. The aid of the above simplified models, and the recent availability of the phonon spectra of solids and relativistic electron wave functions greatly increased the information which could be extracted from the data. The present experiment and analysis then allow a fairly complete and detailed description of germanium impurities imbedded in the host materials. The nuclear properties deduced are in general agreement with the predictions of the pairing plus quadrupole model.

The technique of Coulomb implantation together with easily applied models of the interactions involved, theoretical phonon spectra and electron wave functions, then furnishes a powerful tool for the investigation of phenomena such as radiation damage. The investigation of the γ radiation following implantation by the Mössbauer effect promises to be an increasingly fruitful and significant field.

ACKNOWLEDGMENTS

We gratefully acknowledge the many beneficial discussions with L. D. Roberts and in particular we thank him and T. Tucker for furnishing us with the electron-wave-function calculations for germanium. G. Dolling is to be thanked for making available to us the results of his theoretical investigations of phonon spectra in several materials. The discussions with R. Uher concerning nuclear models and the results of his calculations were greatly appreciated. We thank members of the Oak Ridge National Laboratory Mathematics Division, P. M. Kannan and W. L. McMullen, for helping us with computer calculations.